SCIENCE CHINA
Chemistry

•COMMUNICATIONS•

September 2022 Vol.65 No.9: 1704–1709
https://doi.org/10.1007/s11426-022-1350-1

Substituent engineering in g-C_3N_4/COF heterojunctions for rapid charge separation and high photo-redox activity

Jiayun Guo[1†], Dongge Ma[2†], Fulin Sun[3], Guilin Zhuang[3], Qi Wang[1*], Abdullah M. Al-Enizi[4], Ayman Nafady[4] & Shengqian Ma[5*]

[1]*School of Environmental Science and Engineering, Zhejiang Gongshang University, Hangzhou 310018, China;*
[2]*Department of Chemistry, College of Chemistry and Materials Engineering, Beijing Technology and Business University, Beijing 100048, China;*
[3]*Institute of Industrial Catalysis, College of Chemical Engineering, Zhejiang University of Technology, Hangzhou 310023, China;*
[4]*Department of Chemistry, College of Science, King Saud University, Riyadh 11451, Saudi Arabia;*
[5]*Department of Chemistry, University of North Texas, Denton, TX 76201, USA*

Received June 4, 2022; accepted July 26, 2022; published online August 16, 2022

The heterojunction composed of covalent organic frameworks (COFs) with adjustable structure and other photocatalysts has great potential in the field of photocatalysis. However, effectively enhancing the photocatalytic performance of organic heterojunctions by designing the structure of COFs has not been explored. Herein, TPB-TP-COFs fabricated from 1,3,5-tris(4-amino-phenyl)benzene (TPB) and terephthalaldehyde (TP) with different substituents (−H, −OH, $-OCH_3$, −Br and −F groups), were applied to construct g-C_3N_4/COFs. The performance improvement of the heterojunction could be affected by substituents, and only $-OCH_3$ groups can significantly improve both the photocatalytic phenol oxidation and Cr(VI) reduction. DFT calculation demonstrated that the substituents will affect the electron cloud distribution of CBM, and the location of CBM in the TPB segment is beneficial for the charge transport between TPB-TP-OCH_3 and g-C_3N_4. The enhanced charge transfer from g-C_3N_4 to TPB segment and the improved light absorption of TPB-TP-OCH_3 jointly optimize the photocatalytic redox capacity of g-C_3N_4/TPB-TP-OCH_3. On the basis of this study, regulating the electronic effects of semiconductors played a vital role in improving photocatalytic performance in organic heterojunctions.

monofluorophosphate, g-C_3N_4, heterojunction, photocatalysis, substituent electronegativity

Citation: Guo J, Ma D, Sun F, Zhuang G, Wang Q, Al-enizi AM, Nafady A, Ma S. Substituent engineering in g-C_3N_4/COF heterojunctions for rapid charge separation and high photo-redox activity. *Sci China Chem*, 2022, 65: 1704–1709, https://doi.org/10.1007/s11426-022-1350-1

Photocatalysis, as an eco-friendly chemical approach, has gained widespread attention due to its utilization of renewable solar energy [1−3]. However, the inefficient use of visible light, fast recombination of photo-generated electron-hole (e^--h^+) pairs, and the low charge carrier mobility of traditional semiconductors limit their industrial applications. As the core of photocatalysis, photocatalysts play the key role in its development [4,5]. Since its first discovery, seeking appropriate photocatalysts has been an extensively pursued topic.

Covalent organic frameworks (COFs) are periodically arranged porous crystalline materials possessing high stability and large surface area [6–9]. The peculiar properties of COFs render them great potential for photocatalysis. For example, the long-range ordered structure and periodic π-π stacking can significantly broaden the light absorption, promote the rapid transfer of charge carriers, and inhibit the recombination of photo-generated e^--h^+ pairs [10,11]. The framework and electronic structure of COFs can be designed

†These authors contributed equally to this work.
*Corresponding authors (email: wangqi8327@zjgsu.edu.cn; shengqian.ma@unt.edu)

and adjusted at the molecular level for desired photocatalytic performance [12,13]. In recent years, COFs have been explored for the photocatalytic application of water splitting [14−16], CO_2 reduction [17,18], environmental remediation [19], and organic synthesis [20]. Owing to the diversity of building blocks, it is convenient to fine-tune the photochemical properties of COFs with boosted activity [15,21,22].

Besides, the construction of the heterojunction between COFs and other photocatalysts can serve as a general strategy to further improve the separation efficiency of photogenerated e^--h^+ pairs [23−28]. In particular, the g-C_3N_4 with visible-light response, high stability, and "earth-abundant" nature [29], has been used to construct g-C_3N_4/COFs organic heterojunction [30,31]. Although heterojunctions of g-C_3N_4 and various COFs have been constructed, most studies only focus on the improvement of photocatalytic performance [32−34], while the research on controlling designing the structure of COFs to affect the photocatalytic performance of g-C_3N_4/COFs is still in its infancy.

Herein, we studied the effects of different electronegative substituents of COFs on the improvement of photocatalytic properties (Figure 1). A series of heterostructure photocatalysts comprised of g-C_3N_4 and COFs with different substituents, including −F or −OCH_3, were synthesized. −F acts as electron-withdrawing groups, while −OCH_3 acts as electron-donating groups due to its strong electron-donating conjugation effect. The as-called TPB-TP-H, TPB-TP-F COFs and TPB-TP-OCH_3 were constructed by reacting 1,3,5-tris(4-amino-phenyl)benzene (TPB) with terephthalaldehyde (TP-H), difluoroterephthalaldehyde (TP-F), and dimethoxyterephthaldehyde (TP-OCH_3), respectively. Among these photocatalysts, g-C_3N_4/TPB-TP-OCH_3 exhibited the best photocatalytic performance for phenol degradation and Cr(VI) reduction. The electron-donating ability of −OCH_3 groups enables charge distribution favorable to charge transfer in heterojunctions, which was supported by density functional theory (DFT) calculation, electrochemical measurements and photoluminescence spectra (PL). For the first time, we demonstrated that adjusting the electronic effect of COFs plays an important role in improving the photocatalytic properties of organic heterojunction such as g-C_3N_4/TPB-TP-COFs.

To verify the successful synthesis of g-C_3N_4/TPB-TP-COFs, a series of characterizations were carried out. The refined XRD of TPB-TP-COFs is in good agreement with the experimental results (Figure S1, Supporting Information online). Thus, the similar main peak positions of TPB-TP-COFs indicated that the substituents had little effect on the main crystal structure (Figure 2a). The rather lower crystallinity of TPB-TP-H can be attributed to the aggregation of a large amount of charged groups polarized by imine bond, thus causing electrostatic repulsion and making the layered structure destabilization [35]. TPB-TP-F and TPB-TP-OCH_3 exhibited enhanced crystallinity compared with TPB-TP-H, indicating its improved structural stability. Furthermore, the hybrid materials of g-C_3N_4/TPB-TP-F and g-C_3N_4/TPB-TP-OCH_3 remained prominent diffraction peaks, demonstrating high crystallinity of COFs in the composites. However, there were no significant diffraction peaks of TPB-TP-H in g-C_3N_4/TPB-TP-H due to the relatively low crystallinity of TPB-TP-H. The existence of g-C_3N_4 can be clearly observed after magnifying the peaks of g-C_3N_4/TPB-TP-COFs. Fourier transform infrared (FT-IR) spectroscopy further confirmed the presence of g-C_3N_4 in g-C_3N_4/TPB-TP-COFs (Figure S2), as the triazine stretching was observed at 810 cm^{-1} [36]. The peaks at around 1,650 cm^{-1} and 1,550 cm^{-1} were attributed to the stretching vibration of C=N and C=C bonds which confirmed the formation of imine linkages in TPB-TP-COFs [35]. The scanning electron microscopy (SEM) images of g-C_3N_4/TPB-TP-COFs showed that seaurchin-like TPB-TP-OCH_3 was coated by layered platelet-like g-C_3N_4 (Figure S3).

Nitrogen gas sorption measurements at 77 K indicated that the introduction of both electron donating and withdrawing groups to TPB-TP-COFs could significantly enhance the porosity (Figure 2b, Table S1). The pore size distributions determined by BJH method suggested that the introduction of g-C_3N_4 reduced the pore size of TPB-TP-COFs almost in the same proportion, suggesting that g-C_3N_4 with low porosity did not block the pores of the COFs (Figure S4). Thermogravimetric analysis (TGA) performed in a N_2 atmosphere with 30% O_2 indicated that all the samples exhibited good thermal stability up to 400 °C (Figure S5).

The light-absorbance characteristics conducted on ultraviolet-visible diffuse reflectance spectroscopy (UV-Vis DRS) indicated that the introduction of −OCH_3 group to TPB-TP-COFs can extend light absorption much more than that of −F group (Figure 2c). Thus, TPB-TP-OCH_3 gave rise to the narrowest band gap of 2.42 eV based on the Kubelka-Munk function, which was easier to be excited (Figure S6). The energy band structure of g-C_3N_4 and TPB-TP-COFs including conduction band minimum (CBM) and the corresponding valence band maximum (VBM) was determined by Mott-Schottky plots (Figure S7). The introduction of −F and −OCH_3 substituents reduced the energy direction of VBM and CBM to some extent (Table S2). As a result of the staggered band edge potentials between g-C_3N_4 and TPB-TP-COFs with different substituents, the type II heterojunction can all be successfully formed (Figure 2d).

Phenol and Cr(VI) were selected as model pollutants to evaluate the photocatalytic redox ability of g-C_3N_4/TPB-TP-COFs heterojunction. The first-order model was used to fit the experimental data. It was found that by adjusting the electronic effects of the COF substituents, the performance improvement of the heterojunction could be affected. In this

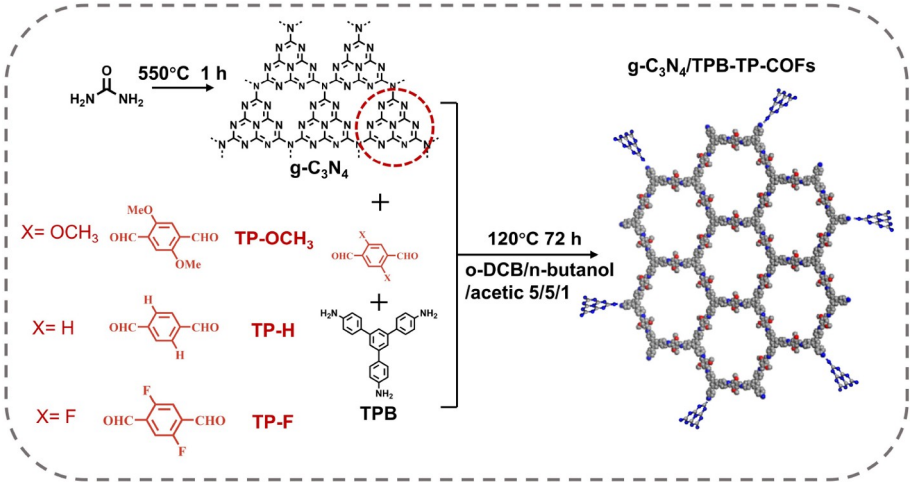

Figure 1 Schematic synthetic route of g-C_3N_4/TPB-TP-COFs with different substituents (color online).

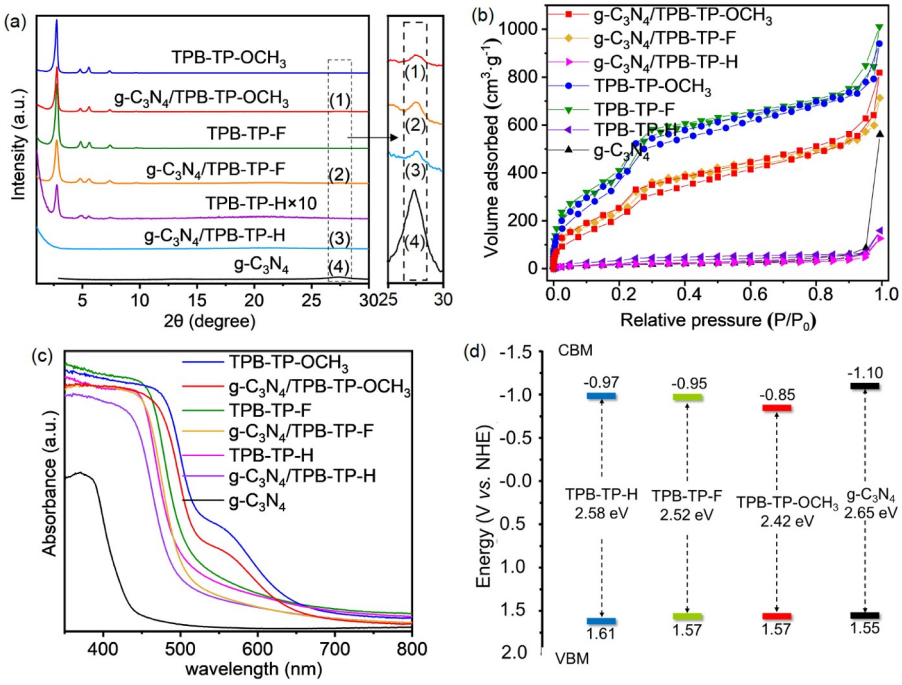

Figure 2 (a) PXRD patterns, (b) N_2 adsorption-desorption isotherms and (c) UV-vis-DRS spectra of g-C_3N_4, TPB-TP-COFs and g-C_3N_4/TPB-TP-COFs. (d) Band position of different TPB-TP-COFs and g-C_3N_4 (color online).

regard, g-C_3N_4/TPB-TP-OCH_3 exhibited enhanced photocatalytic activity for both Cr(VI) reduction and phenol oxidation, thereby demonstrating the best photocatalytic redox activity (Figure 3a,b, Figure S8). However, the heterojunction of g-C_3N_4/TPB-TP-F could merely improve the photocatalytic oxidation rate of phenol, while it had no improvement for photocatalytic Cr(VI) reduction.

It is of great importance to explore the main active species in the photocatalytic reaction to further elaborate the mechanism for this phenomenon. A series of scavengers including ammonium oxalate (act as h^+ scavenger), *tert*-butyl alcohol (TBA, act as HO• scavenger) and benzoquinone (act as $O_2^{\bullet-}$ scavenger) were introduced into the g-C_3N_4/TPB-TP-OCH_3 system (Figure 3c). It was found that $O_2^{\bullet-}$ was the main active species, while h^+ also acted for the phenol degradation. The experiment under N_2 and O_2 atmosphere further proved the role of $O_2^{\bullet-}$ for the phenol degradation. Since the CBM potential of TPB-TP-COFs was more negative than the redox potential of $O_2/O_2^{\bullet-}$ (−0.33 eV *vs.* NHE), the transfer of electrons from the CBM of TPB-TP-OCH_3 to O_2 was thermodynamically feasible, leading to the generation of $O_2^{\bullet-}$ (Figure 3d).

To understand the role of $-OCH_3$ groups in enhancing photocatalytic activity of g-C_3N_4/TPB-TP-OCH_3 hetero-

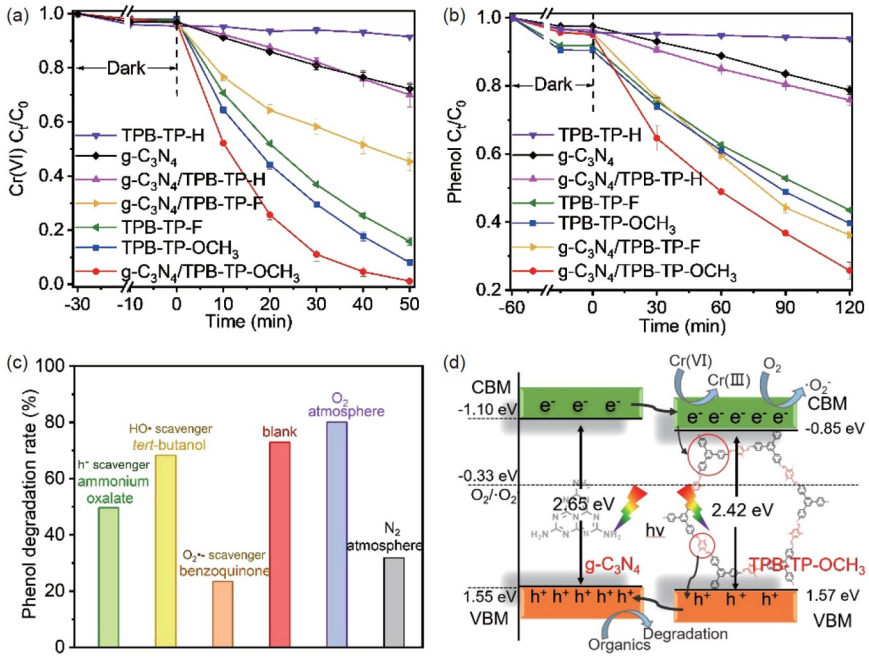

Figure 3 (a) Photocatalytic Cr(VI) reduction and (b) phenol degradation in the presence of g-C_3N_4, TPB-TP-COFs and g-C_3N_4/TPB-TP-COFs. (c) Photocatalytic degradation of phenol over g-C_3N_4/TPB-TP-OCH_3 with different scavengers, under N_2 and O_2 atmosphere. (d) Proposed mechanism of g-C_3N_4/TPB-TP-OCH_3 for removing phenol and Cr(VI) (color online).

junctions, spin-polarization DFT calculation was performed to obtain the possible effects of substituents on electrons moving within the structure. Differential charge density of CBM and VBM of TPB-TP-F, TPB-TP-OCH_3 and TPB-TP-H was calculated, and it was found that substituents have great impact on the CBM of COFs while little impact on VBM of COFs (Figure 4a). The introduction of $-OCH_3$ group allowed the CBM electronic distribution of TPB-TP-OCH_3 to be more extensive and mainly located in the TPB segment. In the g-C_3N_4/TPB-TP-COFs heterojunction, the electrons in the CB of g-C_3N_4 will transfer to the CB of TPB-TP-COFs. Since the CBM of TPB was lower than that of g-C_3N_4 while the CBM of TP was higher than that of g-C_3N_4 [37,38], the photo-excited electrons accumulated in the CB of g-C_3N_4 are inclined to transfer to the lower energy level part, the TPB segment. While the CB of TPB-TP-OCH_3 is mainly located in the TPB segment, it was beneficial for electron transfer from g-C_3N_4 to TPB-TP-OCH_3. Though the introduction of −F could improve the electron-hole separation of TPB-TP-COF, the CBM of TPB-TP-F mainly distributed in the TP segment, which hindered the electron transport to g-C_3N_4. Thus, the difference in the photocatalytic reduction ability of g-C_3N_4/TPB-TP-COFs can be ascribed to the electronic effects of substituents, which influenced the charge density distribution of CBM, resulting in a difference of electron (Figure 4b). The g-C_3N_4/TPB-TP-OCH_3 had higher photocurrent response than pristine TPB-TP-OCH_3, while g-C_3N_4/TPB-TP-F showed a decreased response relative to TPB-TP-F, indicating that the electronegativity of the substituents in COFs will also affect the charge separation ability of the g-C_3N_4/TPB-TP-COF heterojunction. We further introduced −Br and −OH substituents to synthesize porous COFs TPB-TP-Br and TPB-TP-OH (Scheme S1 and Figure S9), and a series of g-C_3N_4/TPB-TP-COFs composites were constructed. It can be seen that apart from g-C_3N_4/TPB-TP-OH, which cannot form the heterojunction (Figure S10), the Cr(VI) reduction effects of g-C_3N_4/TPB-TP-COFs were closely related to the electronegativity of the substituents. The electronegativity of the substituents were as the order of −F > −Br > $-OCH_3$, while g-C_3N_4/TPB-TP-COFs show the opposite effects of Cr(VI) reduction, namely g-C_3N_4/TPB-TP-F < g-C_3N_4/TPB-TP-Br < g-C_3N_4/TPB-TP-OCH_3 (Figure S11), further demonstrating the effects of substituent electronegativity on the electron transfer in the heterojunction. EIS also revealed similar tendency (Figure 4c). That is, g-C_3N_4/TPB-TP-OCH_3 displayed the smallest interfacial charge transfer resistance, indicating quick charge transfer from interface to reactant. Moreover, it also presented the lowest carrier recombination rate according to the PL spectra (Figure 4d). Thus, the charge carries in g-C_3N_4/TPB-TP-OCH_3 can be more effectively generated, separated and transferred for photocatalytic reactions. Based on the above analyses, it can be deduced that the enhanced charge transfer from g-C_3N_4 to TPB-TP-OCH_3 determined the optimal photocatalytic redox capacity of g-C_3N_4/TPB-TP-OCH_3.

The loading ratio of g-C_3N_4 was further optimized in g-C_3N_4/TPB-TP-OCH_3 heterojunction according to the photocatalytic reduction of Cr(VI) and degradation of phenol (Figure S12). Moreover, compared with the reported pho-

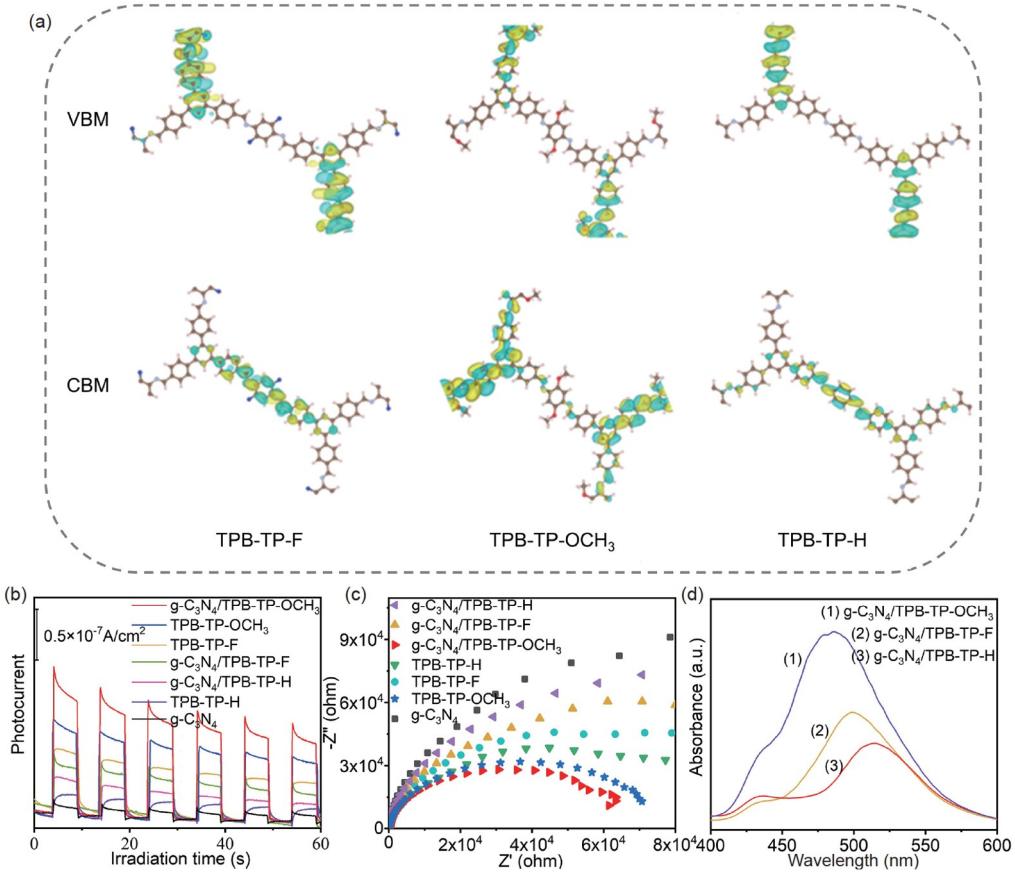

Figure 4 (a) Differential charge densities of CBM and VBM in TPB-TP-F, TPB-TP-OCH_3 and TPB-TP-H. (b) Transient photocurrent response and (c) EIS Nyquist plots of g-C_3N_4, TPB-TP-COFs and g-C_3N_4/TPB-TP-COFs. (d) Photoluminescence spectra of different g-C_3N_4/TPB-TP-COFs (color online).

tocatalysts (including TiO_2, C_3N_4, MOFs, COFs and their composites), the optimal g-C_3N_4/TPB-TP-OCH_3 maintained excellent redox effects under the condition of low catalyst concentration (Table S3). The optimal g-C_3N_4/TPB-TP-OCH_3 also exhibited high stability both in performance and structure (XRD, IR and BET) after six repetitive cycles for the Cr(VI) reduction (Figure S13).

In summary, we constructed g-C_3N_4/TPB-TP-COFs using TPB-TP-COFs with different substituents to illustrate the effects of electronegativity of COFs substituents on the photocatalytic performance of g-C_3N_4/TPB-TP-COFs. It was demonstrated that changing the substituents can tune the electron cloud distribution on CBM and VBM of COFs, thus affecting the charge transport efficiency with g-C_3N_4. The electron-donating group (−OCH_3) was superior to electron-withdrawing group (−F). The as-prepared g-C_3N_4/TPB-TP-OCH_3 heterojunction displayed boosted performance than g-C_3N_4/TPB-TP-F and g-C_3N_4/TPB-TP-H. The superior catalytic efficiency of g-C_3N_4/TPB-TP-OCH_3 can be attributed to the improved light absorption as well as the enhanced charge transfer from g-C_3N_4 to TPB segment. This work demonstrated that in organic heterojunctions, regulating the electronic effect of semiconductors plays a crucial role in improving photocatalytic performance, which was a key for designing organic heterojunctions with high photocatalytic properties.

Acknowledgements This work was supported by the National Natural Science Foundation of China (21876154) and the Fundamental Research Funds for the Provincial Universities of Zhejiang (JRK22001). Partially support from the Robert A. Welch Foundation (B-0027) (SM) and the Researchers Supporting Program (RSP-2022/55) at King Saud University, Riyadh, Saudi Arabia (AMA) is also acknowledged.

Conflict of interest The authors declare no conflict of interest.

Supporting information The supporting information is available online at http://chem.scichina.com and http://link.springer.com/journal/11426. The supporting materials are published as submitted, without typesetting or editing. The responsibility for scientific accuracy and content remains entirely with the authors.

1 Song X, Wei G, Sun J, Peng C, Yin J, Zhang X, Jiang Y, Fei H. *Nat Catal*, 2020, 3: 1027–1033
2 Zhang G, Lan ZA, Wang X. *Angew Chem Int Ed*, 2016, 55: 15712–15727
3 Lin L, Lin Z, Zhang J, Cai X, Lin W, Yu Z, Wang X. *Nat Catal*, 2020, 3: 649–655
4 Zhang K, Fu Y, Hao D, Guo J, Ni BJ, Jiang B, Xu L, Wang Q. *J Alloys Compd*, 2022, 891: 161994
5 Fu Y, Zhang K, Zhang Y, Cong Y, Wang Q. *Chem Eng J*, 2021, 412: 128722
6 Segura JL, Mancheño MJ, Zamora F. *Chem Soc Rev*, 2016, 45: 5635–

5671
7 Vardhan H, Nafady A, Al-Enizi AM, Ma S. *Nanoscale*, 2019, 11: 21679–21708
8 Rodríguez-San-Miguel D, Montoro C, Zamora F. *Chem Soc Rev*, 2020, 49: 2291–2302
9 Lu M, Zhang M, Liu CG, Liu J, Shang LJ, Wang M, Chang JN, Li SL, Lan YQ. *Angew Chem Int Ed*, 2021, 60: 4864–4871
10 Zhao Y, Dai W, Peng Y, Niu Z, Sun Q, Shan C, Yang H, Verma G, Wojtas L, Yuan D, Zhang Z, Dong H, Zhang X, Zhang B, Feng Y, Ma S. *Angew Chem Int Ed*, 2020, 59: 4354–4359
11 Shi JL, Chen R, Hao H, Wang C, Lang X. *Angew Chem Int Ed*, 2020, 59: 9088–9093
12 Meng Y, Luo Y, Shi JL, Ding H, Lang X, Chen W, Zheng A, Sun J, Wang C. *Angew Chem Int Ed*, 2020, 59: 3624–3629
13 Wang S, Sun Q, Chen W, Tang Y, Aguila B, Pan Y, Zheng A, Yang Z, Wojtas L, Ma S, Xiao FS. *Matter*, 2020, 2: 416–427
14 Vyas VS, Haase F, Stegbauer L, Savasci G, Podjaski F, Ochsenfeld C, Lotsch BV. *Nat Commun*, 2015, 6: 8508
15 Bi S, Yang C, Zhang W, Xu J, Liu L, Wu D, Wang X, Han Y, Liang Q, Zhang F. *Nat Commun*, 2019, 10: 2467
16 Jin E, Lan Z, Jiang Q, Geng K, Li G, Wang X, Jiang D. *Chem*, 2019, 5: 1632–1647
17 Gong YN, Zhong W, Li Y, Qiu Y, Zheng L, Jiang J, Jiang HL. *J Am Chem Soc*, 2020, 142: 16723–16731
18 Lu M, Liu J, Li Q, Zhang M, Liu M, Wang JL, Yuan DQ, Lan YQ. *Angew Chem Int Ed*, 2019, 58: 12392–12397
19 He S, Yin B, Niu H, Cai Y. *Appl Catal B-Environ*, 2018, 239: 147–153
20 Chen R, Shi JL, Ma Y, Lin G, Lang X, Wang C. *Angew Chem Int Ed*, 2019, 58: 6430–6434
21 Stegbauer L, Zech S, Savasci G, Banerjee T, Podjaski F, Schwinghammer K, Ochsenfeld C, Lotsch BV. *Adv Energy Mater*, 2018, 8: 1703278
22 Yin L, Zhao Y, Xing Y, Tan H, Lang Z, Ho W, Wang Y, Li Y. *Chem Eng J*, 2021, 419: 129984
23 Zhang M, Lu M, Lang ZL, Liu J, Liu M, Chang JN, Li LY, Shang LJ, Wang M, Li SL, Lan YQ. *Angew Chem Int Ed*, 2020, 59: 6500–6506
24 Jiang Q, Sun L, Bi J, Liang S, Li L, Yu Y, Wu L. *ChemSusChem*, 2018, 11: 1108–1113
25 Li Y, Karimi M, Gong YN, Dai N, Safarifard V, Jiang HL. *Matter*, 2021, 4: 2230–2265
26 Zhang M, Chang JN, Chen Y, Lu M, Yu TY, Jiang C, Li SL, Cai YP, Lan YQ. *Adv Mater*, 2021, 33: 2105002
27 Peng Y, Zhao M, Chen B, Zhang Z, Huang Y, Dai F, Lai Z, Cui X, Tan C, Zhang H. *Adv Mater*, 2018, 30: 1705454
28 Zhang FM, Sheng JL, Yang ZD, Sun XJ, Tang HL, Lu M, Dong H, Shen FC, Liu J, Lan YQ. *Angew Chem Int Ed*, 2018, 57: 12106–12110
29 Ong WJ, Tan LL, Ng YH, Yong ST, Chai SP. *Chem Rev*, 2016, 116: 7159–7329
30 Luo M, Yang Q, Liu K, et al. *ChemComm*, 2019, 55: 5829–5832
31 Hou Y, Cui CX, Zhang E, Wang JC, Li Y, Zhang Y, Zhang Y, Wang Q, Jiang J. *Dalton Trans*, 2019, 48: 14989–14995
32 Yao Y, Hu Y, Hu H, Chen L, Yu M, Gao M, Wang S. *J Colloid Interface Sci*, 2019, 554: 376–387
33 Xing Y, Wang X, Hao S, Zhang X, Wang X, Ma W, Zhao G, Xu X. *Chin Chem Lett*, 2021, 32: 13–20
34 Wang L, Lian R, Zhang Y, Ma X, Huang J, She H, Liu C, Wang Q. *Appl Catal B-Environ*, 2022, 315: 121568
35 Xu H, Gao J, Jiang D. *Nat Chem*, 2015, 7: 905–912
36 Liu J, Zhang T, Wang Z, Dawson G, Chen W. *J Mater Chem*, 2011, 21: 14398–14401
37 Xu C, Liu X, Li D, Chen Z, Yang J, Huang J, Pan H. *ACS Appl Mater Interfaces*, 2021, 13: 20114–20124
38 Tian J, Zhang L, Fan X, Zhou Y, Wang M, Cheng R, Li M, Kan X, Jin X, Liu Z, Gao Y, Shi J. *J Mater Chem A*, 2016, 4: 13814–13821